

DEM SIMULATIONS OF DYNAMIC ANGLE OF REPOSE OF ACEROLA RESIDUE: A PARAMETRIC STUDY USING A RESPONSE SURFACE TECHNIQUE

K. G. SANTOS¹, A. V. P. CAMPOS², O. S. OLIVEIRA², L. V. FERREIRA²,
M. C. FRANCISQUETTI², M. A. S. BARROZO²

¹ Universidade Federal do Triângulo Mineiro, Departamento de Engenharia Química

² Universidade Federal de Uberlândia, Faculdade de Engenharia Química

E-mail para contato: kassiagsantos@gmail.com

RESUMO – In the present work, some fluid-dynamics aspects of a rotary drum, operating with acerola residue particles were investigated experimentally and by DE Discret Elements Method (DEM). In order to evaluate the effect of parameters of the JKR contact force model on the dynamic angle of repose, a central composite design was used to plan the DEM simulations, performed by EDEM software. The simulated dynamic angles of repose were compared with the experimental one and it were selected the parameters the better represent the fluid dynamic behavior of the acerola residue particles.

1. INTRODUCTION

Today, thanks to rapid advances in computational science, studies involving numerical simulation have become popular in the field of gas-solid flows and can help increase our understanding about the fluid dynamic behavior of particle in diverse types of equipments (Santos et al, 2009). Discrete Element Modeling (DEM) is a numerical tool that models a granular system as an assembly of discrete particles that interact with each other and with any other solid body, such as the vessel wall (Bortolotti *et al.*, 2013).

Cundall and Strack (1975) first proposed the discrete element method to model the motion of granular material. Ever since, granular flows have been reproduced successfully by DEM simulations of many processes, including hopper discharge; rotating drum; flat blade mixer; static angle of repose; dynamic angle of repose; packing bed; fluidized bed; spouted bed; granulator; dense cyclone¹ and coating of pharmaceutical tablets.

The DEM technique usually requires a previous calibration of parameters using a simple system that characterizes the flowability of granular materials, like the dynamic angle of repose. This angle is related to the particle density, surface area and shape, and the coefficient of friction of the material. Knowledge about the angle of repose can help shed light on the fluid dynamic behavior of material and consist in the first step for future applications of DEM simulations in moving beds. This study investigated the fluid dynamics of acerola residue in a rotary vessel. Several DEM simulations were performed to reproduce the dynamic angle of repose for acerola residue particles. A comparison was made of the simulated and experimental results.

2. DEM SIMULATIONS

DEM simulations involve following the motion of every particle in the flow and modeling each collision between combinations of particles and between particles and their environment. The general DEM methodology and its variants are well established and are described in greater detail by Cleary (1998). The contact between two smooth elastic bodies was investigated by Hertz (1882), who demonstrated that both the size and shape of the zone of contact followed from the elastic deformation of the bodies.

The *Hertz-Mindlin* model combined with the *JKR* cohesive model was used to account the cohesive force in the particles collision (Bortolotti *et al.*, 2013). In the *Hertz-Mindlin* model, the normal force component is based on Hertzian contact theory. Both normal and tangential forces have damping components, with the damping coefficient related to the coefficient of restitution, as described by Tsuji *et al.* (1992). The tangential component of the friction force follows Coulomb's friction law. The rolling friction is implemented as the directional torque constant model. The normal force (F_n) is a function of normal overlap (δ_n) and is given by:

$$F_n = \frac{4}{3} E^* \sqrt{R^*} \delta_n^{3/2} \quad (1)$$

where the equivalent Young Modulus (E^*) and the equivalent radius (R^*) are defined as:

$$\frac{1}{E^*} = \frac{(1-\nu_i^2)}{E_i} + \frac{(1-\nu_j^2)}{E_j} \quad (2)$$

$$\frac{1}{R^*} = \frac{1}{R_i} + \frac{1}{R_j} \quad (3)$$

where E_i , ν_i , R_i and E_j , ν_j , R_j are the Young Modulus, Poisson ratio and radius of each particle in contact. Additionally, there is a damping force (F_n^d) given by:

$$F_n^d = -2\sqrt{\frac{5}{6}} \left[\frac{\ln e}{\sqrt{\ln^2 e + \pi^2}} \right] \sqrt{(2E^* \sqrt{R^*} \delta_n) m^* v_n^{rel}} \quad (4)$$

where $m^* = (m_i^{-1} + m_j^{-1})^{-1}$ is the equivalent mass, v_n^{rel} is the normal component of the relative velocity, and e is the coefficient of restitution. The tangential force F_t depends on the tangential overlap (δ_t) and tangential stiffness (S_t).

$$F_t = -\delta_t S_t = -\delta_t 8G^* \sqrt{R^*} \delta_n \quad (5)$$

where G^* is the equivalent shear modulus. The tangential damping is given by:

$$F_t^d = -2\sqrt{\frac{5}{6}} \left[\frac{\ln e}{\sqrt{\ln^2 e + \pi^2}} \right] \sqrt{S_t m^* v_t^{rel}} \quad (6)$$

where v_t^{rel} is the relative tangential velocity. The tangential force is limited by Coulomb friction $\mu_s F_n$, where μ_s is the coefficient of static friction.

For simulations in which rolling friction is important, this is accounted for by applying a torque to the contact surfaces:

$$\tau_i = -\mu_r F_n R_i \omega_i \quad (7)$$

where μ_r is the coefficient of rolling friction, R_i is the distance of the contact point from the center of mass and ω_i is the unit angular velocity vector of the object at the contact point.

The *Hertz-Mindlin* model combined with the *JKR* model is a cohesion contact model that accounts for the influence of van der Waals forces within the contact zone and allows one to model strongly adhesive systems, such as dry powders or wet materials (Mindlin, 1949). The *JKR* model is used here to represent the influence of various cohesive effects in a simplified way. This model uses the same calculations as the *Hertz-Mindlin* contact model to represent the tangential elastic force, the normal dissipation force, and the tangential dissipation force. To account for cohesion, the normal elastic contact force (F_{JKR}) is based on the Johnson-Kendall-Roberts theory reported by Johnson *et al.* (1971). This force depends on the overlap (δ) and on the interaction parameter, surface energy (γ), as follows:

$$F_{JKR} = -4\sqrt{\pi\gamma E^*} a^{3/2} + \frac{4E^*}{3R^*} a^3 \quad (8)$$

$$\delta = \frac{a^2}{R^*} - \sqrt{4\pi\gamma a / E^*} \quad (9)$$

When cohesion is not an important force ($\gamma = 0$), the F_{JKR} force becomes a normal Hertz-Mindlin force (F_n). The *JKR* model provides attractive cohesion forces even if the particles are not in physical contact. The maximum gap between particles with non-zero force is given by:

$$\delta_c = \frac{a_c^2}{R^*} - \sqrt{4\pi\gamma a_c / E^*} \quad (10)$$

$$a_c = \left[\frac{9\pi\gamma R^{*2}}{2E^*} \left(\frac{3}{4} - \frac{1}{\sqrt{2}} \right) \right]^{\frac{1}{3}} \quad (11)$$

For $\delta < \delta_c$ the model returns zero force. The cohesion force reaches its maximum value when the particles are not in physical contact and the separation gap is less than δ_c (reference). The value of maximum cohesion force, called pull-out force, is given by:

$$F_{pull-out} = -\frac{3}{2}\pi\gamma R^* \quad (12)$$

In the *JKR* cohesive model, the friction force depends on the positive repulsive part of the normal *JKR* force. As a result, the *JKR* friction model provides higher friction force when the cohesion component of the contact force is higher.

3. MATERIALS AND METHODS

3.1. Experimental Procedure

The acerola residue (seeds) used in the experiments came from industrial pulp and juice processing by Nettare, a food processing company located in the state of Minas Gerais, southeastern Brazil). Particle size (d_p) and apparent density were measured by the pycnometer method using petroleum ether. The sphericity was measured using a HAVER CPA 3-2 photo-optical particle size analyzer.

Table 1 describes the properties of the material. The dynamic angle of repose was determined by the rotary drum method (Pozitano and Rocha, 2011) in a cylinder with a 0.1 m diameter. This methodology consists of mechanically spinning the cylinder at a constant angular velocity and measuring the angle at which the particles repose (by image analysis). All the measurements were taken in triplicate.

3.2. DEM Simulations

The dynamic angle of repose (Φ) for acerola residue was reproduced by DEM simulations, using EDEM 2.3 software. The time step in all the simulations was fixed at 20% of the critical time step calculated from Rayleigh time.

The behavior of granular materials is strongly dependent on their size and shape; therefore, appropriate modeling of particle shape is very important. In the simulations performed in this study, the shape of the acerola residue were an approximation to the true shape determined by the multisphere method (Favier *et al.*, 1999), as showed in Figure 1. Each particle was generated by twelve spheres. The mean volume of the acerola particle was $3.24 \cdot 10^{-7} \text{ m}^3$.

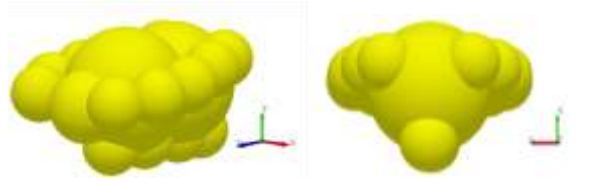


Figure 1 – Shape of the acerola residue determined by the multisphere method

The contact model of Hertz-Mindlin with JKR model, described previously, represented the contact force for the residue particles. In order to evaluate the effect of these model parameters on the dynamic angle of repose, the simulations conditions were chosen using a central composite design with 5 variables and one replicate at the central level. The parameters evaluated were the shear modulus, coefficient of restitution, coefficient of static friction, coefficient of rolling friction and interface energy (cohesion), according with Table 2. The range of parameter values were based on the wide range found in the literature and the variable levels can be found in Table 3. Thus, not all combinations of parameters necessarily lead to physically consistent results, but may contribute to verify the effect of the individual parameter and their interactions on responses. The number of particles used in simulations was constant and corresponded to the total weight of particles in the experiments, as shown in Table 1.

Table 1 – Proprieties of Acerola residue particles and experimental conditions

d_p [mm]	Particle diameter	7.83 ± 0.13
ρ_{ap} [kg/m ³]	Apparent density	738 ± 28
ρ_{real} [kg/m ³]	Real density	1344.85 ± 13.86
ϕ	Sphericity	0.68 ± 0.02
N	Number of particles inside the rotary drum	627
v [rpm]	Rotational Speed	25
D [m]	Diameter of rotary drum	0.1

4. RESULTADOS

In this work, the dynamic angle of repose of acerola residue was experimentally measured and simulated by DEM. These parameters can help shed light on the fluid dynamic behavior of these materials in moving beds. Table 2 presents the simulations results performed with the set of parameters defined by the central composite design. It can be seen a significant difference on the simulated dynamic angles of repose, indicating the influence of the studied parameters on response. The runs 16, 20 and 25 conducted to the best agreement with experimental angle of repose (52.6°), with a prediction error of less than 1%. Some simulations (marked with * at Table 2) showed inconsistent results, with a complete particle slipping at wall and so much cohesion between particles. Figure 2(a) compares the experiment and the best simulations data for the angle of repose of acerola residue (run 16 and 25), while the Figure 2 (b) shows the simulations that presents the higher deviation according experimental data. The high dynamic angle of repose of the fruit residues also expresses the low flowability of this material.

Table 2 – Central composite design for parameters evaluation and results of dynamic angle of repose (with a constant Poisson ratio parameter as 0.25)

Simulation	Shear Modulus [Pa]	Coefficient of Restitution	Coefficient of Static Friction	Coefficient of Rolling Friction	Interface Energy [J/m ²]	Φ_{DEM}	σ [%]
Run 1*	-1.000	-1.000	-1.000	-1.000	1.000	46.24 ±0.99	12.03
Run 2*	-1.000	-1.000	-1.000	1.000	-1.000	50.53 ±0.48	3.87
Run 3	-1.000	-1.000	1.000	-1.000	-1.000	49.63 ±1.95	5.57
Run 4	-1.000	-1.000	1.000	1.000	1.000	61.11 ±4.00	-16.27
Run 5*	-1.000	1.000	-1.000	-1.000	-1.000	40.03 ±1.13	23.84
Run 6*	-1.000	1.000	-1.000	1.000	1.000	43.67 ±1.37	16.92
Run 7	-1.000	1.000	1.000	-1.000	1.000	47.19 ±1.98	10.22
Run 8	-1.000	1.000	1.000	1.000	-1.000	57.67 ±1.52	-9.72
Run 9*	1.000	-1.000	-1.000	-1.000	-1.000	42.71 ±2.17	18.73
Run 10*	1.000	-1.000	-1.000	1.000	1.000	54.29 ±1.82	-3.28
Run 11	1.000	-1.000	1.000	-1.000	1.000	51.22 ±3.67	2.55
Run 12	1.000	-1.000	1.000	1.000	-1.000	61.27 ±2.98	-16.58
Run 13	1.000	1.000	-1.000	-1.000	1.000	47.00 ±3.34	10.57
Run 14*	1.000	1.000	-1.000	1.000	-1.000	55.88 ±1.13	-6.32
Run 15	1.000	1.000	1.000	-1.000	-1.000	53.92 ±1.26	-2.58
Run 16	1.000	1.000	1.000	1.000	1.000	52.23 ±3.89	0.63
Run 17	-1.607	0.000	0.000	0.000	0.000	60.15 ±2.16	-14.44
Run 18	1.607	0.000	0.000	0.000	0.000	57.41 ±2.37	-9.22
Run 19	0.000	-1.607	0.000	0.000	0.000	54.91 ±3.38	-4.46
Run 20	0.000	1.607	0.000	0.000	0.000	52.94 ±0.70	-0.73
Run 21*	0.000	0.000	-1.607	0.000	0.000	6.88 ±0.45	86.91
Run 22	0.000	0.000	1.607	0.000	0.000	48.68 ±1.54	7.38
Run 23	0.000	0.000	0.000	-1.607	0.000	47.52 ±2.13	9.59
Run 24	0.000	0.000	0.000	1.607	0.000	63.95 ±1.59	-21.68
Run 25	0.000	0.000	0.000	0.000	-1.607	52.33 ±3.51	0.44
Run 26	0.000	0.000	0.000	0.000	1.607	53.11 ±2.51	1.05
Run 27	0.000	0.000	0.000	0.000	0.000	53.61 ±2.44	-1.99
Run 28	0.000	0.000	0.000	0.000	0.000	55.16 ±2.30	-4.94

* Inconsistent simulation results (particles showed so much cohesion). Run 21 showed strongly numeric inconsistent and it was removed from statistic analysis.

Table 3 – Levels and range values of coded variables

Level	Shear Modulus [Pa]	Coefficient of Restitution	Coefficient of Static Friction	Coefficient of Rolling Friction	Interface Energy [J/m ²]
-1.607	1.178 10 ⁶	0.018	0.018	0.004	0.002
-1.000	3.000 10 ⁶	0.200	0.200	0.050	0.024
0.000	6.000 10 ⁶	0.500	0.500	0.125	0.060
+1.000	9.000 10 ⁶	0.800	0.800	0.200	0.096
+1.607	1.082 10 ⁷	0.982	0.982	0.246	0.118

The combined simulations results served as the basis for a global statistical analysis. A multiple regression analysis was performed to quantify the effect of the parameters of JKR Model on the dynamic angle of repose. To obtain the equation that describes the response as a function of the independent variables, hypothesis tests were performed using the t of Student statistic to identify the significant parameters. The parameters estimated by the least squares method with a significance level higher than 10%, ($p > 0.1$) were neglected. The fitted equation for the simulated dynamic angle of repose (Φ_{DEM}), in matrix notation, is given by ($R^2=0.915$):

$$\Phi_{DEM} = 54.731 + X' \begin{bmatrix} 0.000 \\ -1.066 \\ 0.000 \\ 4.021 \\ 0.000 \end{bmatrix} + X' \begin{bmatrix} 1.691 & 0.578 & 0.794 & 0.000 & 0.000 \\ 0.578 & 0.000 & 0.000 & -0.075 & -0.816 \\ 0.794 & 0.000 & -8.502 & 0.000 & 0.000 \\ 0.000 & -0.075 & 0.000 & 0.000 & -0.607 \\ 0.000 & -0.816 & 0.000 & -0.607 & 0.000 \end{bmatrix} X \quad (13)$$

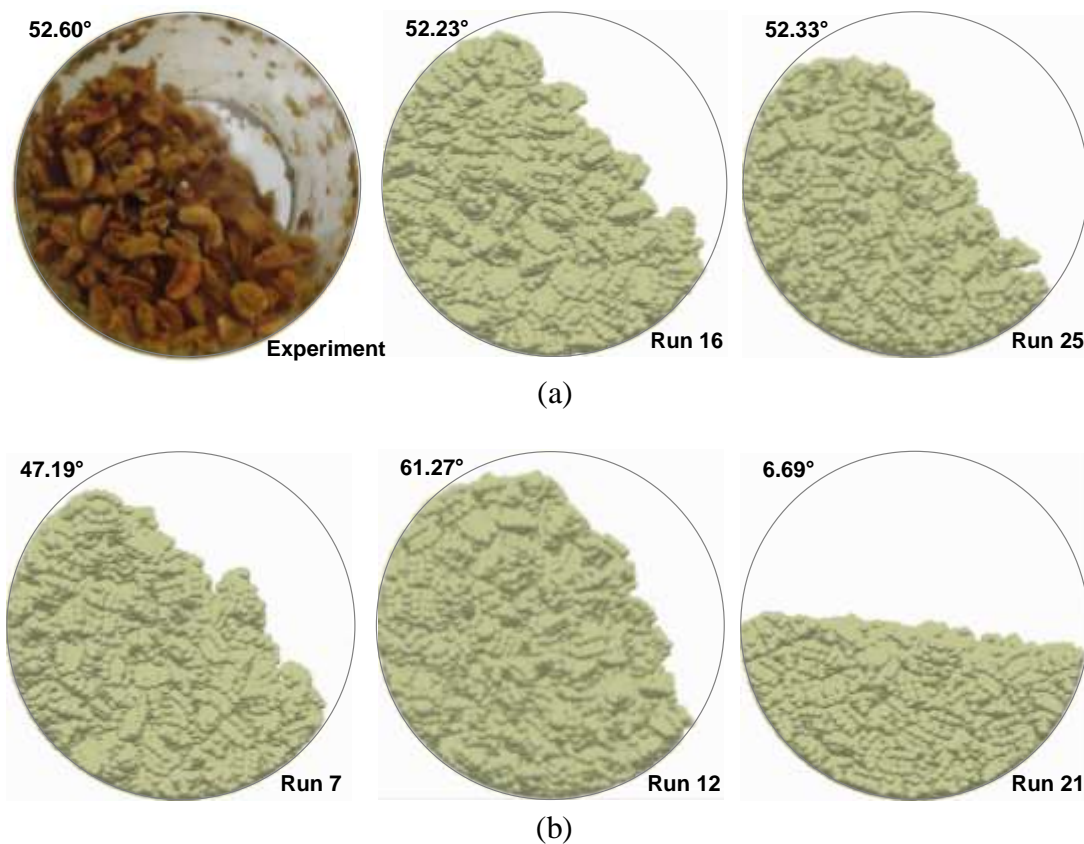


Figure 2 - Dynamic angle of repose of acerola residue particles: (a) comparison between experimental data and best simulations; (b) simulations with higher deviation of experimental data.

The values of the parameters (Equation 13) indicate that the coefficients of static friction and rolling friction are the parameters that most influence the fluid dynamic behavior of particles. Although the interface energy are not significant in the single form, the interactions of this parameter with coefficients of restitution and rolling friction are significant. So, in order to ensure the higher performance of the particle fluid dynamic in simulations, it is extremely important measure experimentally the coefficient of static friction and the other significant parameters which constitute the contact force model employed in DEM simulations.

5. CONCLUSION

In this work, the dynamic angle of response of acerola residue particles was obtained experimentally and by DEM simulations. In order to evaluate the effect of the parameters of Hertz-Mindlin model for the contact force between particles, a central composite design was proposed to plan the simulations. A set of parameters were identified to represent the granular flow of acerola residue particles (runs 16, 20 and 25). The results analysis showed that there is a significant effect of all parameters, according Equation 13, and the coefficients of static friction and rolling friction are the most significant. Thus, a carefully study have been done in order to obtain this parameters to individual material experimentally and improve the DEM simulations results.

6. ACKNOWLEDGMENT

The authors acknowledge the financial support provided by FAPEMIG (PCE-00201-14).

7. REFERENCES

- BORTOLOTTI, C. T.; SANTOS, K. G.; FRANCISQUETTI, M. C. C.; DUARTE, C. R.; BARROZO, M. A. S. Hydrodynamic Study of a Mixture of West Indian Cherry Residue and Soybean Grains in a Spouted Bed. *Can. J. Chem. Eng.*, v. 91, p. 1871-1880, 2013.
- CLEARY, P. W. Predicting charge motion, power draw, segregation and wear in ball mills using discrete element methods, *Min. Eng.*, v. 11, p. 1061, 1998.
- CUNDALL, P. A.; STRACK, O. D. A discrete numerical model for granular assemblies. *Geotechnique*. v. 29, p. 47-65, 1979.
- FAVIER, J.F., ABBASPOUR-FARD, M.H., KREMMER, M., RAJI, A., Shape representation of axi-symmetrical, non-spherical particles in discrete element simulation using multi-element model particles. *Eng. Computations*, v. 6, p. 467- 480, 1999.
- HERTZ, H. On the contact of elastic solids. *J. reine und angewandte Mathematik*, v. 92, p. 156-171, 1882.
- JOHNSON, K. L.; KENDALL, K.; ROBERTS, D. Surface Energy and the Contact of Elastic Solids. *Proc. R. Soc. Lond. A. ou Proceedings of the Royal Society of London. Series A, Mathematical and Physical Sciences*, v. 324, p. 301-313, 1971.
- MINDLIN, R.D. Compliance of elastic bodies in contact. *J. Appl. Mech.*, v. 16, p. 259-268, 1949.
- POZITANO, M.; ROCHA, S. C. S. Caracterização física e germinação de sementes de Senna macranthera. *Rev. Bras. Sem.*, v. 33, p. 777-784, 2011.
- SANTOS, K. G.; MURATA, V. V.; BARROZO, M. A. S. Three-dimensional computational fluid dynamics modeling of spouted bed. *Can. J. Chem. Eng.*, v. 87, p. 211-219, 2009.
- TSUJI, Y., TANAKA, T.; ISHIDA, T. Lagrangian numerical simulation of plug flow of cohesionless particles in a horizontal pipe. *Powder Technol.*, v. 71, p. 239-250, 1992.